Theses and Dissertations   1. Thesis and Dissertation Collection, all items

2019-12

THERMOACOUSTIC PERFORMANCE OF CARBON NANOTUBE SHEETS

Furgiuele, Sean M.

Monterey, CA; Naval Postgraduate School

http://hdl.handle.net/10945/64158

NAVAL
POSTGRADUATE
SCHOOL

MONTEREY, CALIFORNIA

THESIS

**THERMOACOUSTIC PERFORMANCE OF
CARBON NANOTUBE SHEETS**

by

Sean M. Furgiuele

December 2019

Thesis Advisor:	Dragoslav Grbovic
Second Reader:	Bruce C. Denardo

THIS PAGE INTENTIONALLY LEFT BLANK

REPORT DOCUMENTATION PAGE		*Form Approved OMB No. 0704-0188*

Public reporting burden for this collection of information is estimated to average 1 hour per response, including the time for reviewing instruction, searching existing data sources, gathering and maintaining the data needed, and completing and reviewing the collection of information. Send comments regarding this burden estimate or any other aspect of this collection of information, including suggestions for reducing this burden, to Washington headquarters Services, Directorate for Information Operations and Reports, 1215 Jefferson Davis Highway, Suite 1204, Arlington, VA 22202-4302, and to the Office of Management and Budget, Paperwork Reduction Project (0704-0188) Washington, DC 20503.

1. AGENCY USE ONLY (*Leave blank*)	2. REPORT DATE December 2019	3. REPORT TYPE AND DATES COVERED Master's thesis	
4. TITLE AND SUBTITLE THERMOACOUSTIC PERFORMANCE OF CARBON NANOTUBE SHEETS		5. FUNDING NUMBERS	
6. AUTHOR(S) Sean M. Furgiuele			
7. PERFORMING ORGANIZATION NAME(S) AND ADDRESS(ES) Naval Postgraduate School Monterey, CA 93943-5000		8. PERFORMING ORGANIZATION REPORT NUMBER	
9. SPONSORING / MONITORING AGENCY NAME(S) AND ADDRESS(ES) N/A		10. SPONSORING / MONITORING AGENCY REPORT NUMBER	
11. SUPPLEMENTARY NOTES The views expressed in this thesis are those of the author and do not reflect the official policy or position of the Department of Defense or the U.S. Government.			
12a. DISTRIBUTION / AVAILABILITY STATEMENT Approved for public release. Distribution is unlimited.		12b. DISTRIBUTION CODE A	

13. ABSTRACT (maximum 200 words)

Thin carbon nanotube (CNT) sheets are excellent materials for small thermoacoustic (TA) devices. They are strong, lightweight, and can be used to produce sound efficiently through high frequency temperature fluctuations. These TA devices have the potential to be used in active noise cancellation, or as SONAR projectors for very small unmanned underwater vehicles. This thesis aims to evaluate the TA performance of CNT sheets and compare them to theoretical calculations and to other state-of-the-art TA materials. The CNT sheets tested were two Miralon® sheets provided by Nanocomp; one with a density of 10–15 grams per square meter and another with a density of 20–30 grams per square meter. Performance was evaluated based on sound pressure level (SPL) recorded over a frequency range of 500 Hz to 100 kHz. The lower-density sheet was found to have the better performance of the two. Further testing showed that this lower-density sheet has comparable TA performance to other CNT-based materials used for thermophones. The Miralon® sheets are a viable material for use in thermophones and other thermoacoustic devices such as lightweight SONAR projectors.

14. SUBJECT TERMS carbon nanotubes, thermoacoustics, acoustics			15. NUMBER OF PAGES 61
			16. PRICE CODE
17. SECURITY CLASSIFICATION OF REPORT Unclassified	18. SECURITY CLASSIFICATION OF THIS PAGE Unclassified	19. SECURITY CLASSIFICATION OF ABSTRACT Unclassified	20. LIMITATION OF ABSTRACT UU

NSN 7540-01-280-5500

Standard Form 298 (Rev. 2-89)
Prescribed by ANSI Std. 239-18

THIS PAGE INTENTIONALLY LEFT BLANK

THERMOACOUSTIC PERFORMANCE OF CARBON NANOTUBE SHEETS

Sean M. Furgiuele
Ensign, United States Navy
BS, Georgia Institute of Technology, 2018

Submitted in partial fulfillment of the
requirements for the degree of

MASTER OF SCIENCE IN ENGINEERING ACOUSTICS

from the

**NAVAL POSTGRADUATE SCHOOL
December 2019**

Approved by: Dragoslav Grbovic
                Advisor

                Bruce C. Denardo
                Second Reader

                Oleg A. Godin
                Chair, Department of Engineering Acoustics Academic Committee

THIS PAGE INTENTIONALLY LEFT BLANK

ABSTRACT

Thin carbon nanotube (CNT) sheets are excellent materials for small thermoacoustic (TA) devices. They are strong, lightweight, and can be used to produce sound efficiently through high frequency temperature fluctuations. These TA devices have the potential to be used in active noise cancellation, or as SONAR projectors for very small unmanned underwater vehicles. This thesis aims to evaluate the TA performance of CNT sheets and compare them to theoretical calculations and to other state-of-the-art TA materials. The CNT sheets tested were two Miralon® sheets provided by Nanocomp; one with a density of 10–15 grams per square meter and another with a density of 20–30 grams per square meter. Performance was evaluated based on sound pressure level (SPL) recorded over a frequency range of 500 Hz to 100 kHz. The lower-density sheet was found to have the better performance of the two. Further testing showed that this lower-density sheet has comparable TA performance to other CNT-based materials used for thermophones. The Miralon® sheets are a viable material for use in thermophones and other thermoacoustic devices such as lightweight SONAR projectors.

THIS PAGE INTENTIONALLY LEFT BLANK

TABLE OF CONTENTS

LIST OF FIGURES

x

THIS PAGE INTENTIONALLY LEFT BLANK

LIST OF TABLES

THIS PAGE INTENTIONALLY LEFT BLANK

LIST OF ACRONYMS AND ABBREVIATIONS

AC   alternating current

CNT   carbon nanotube

dBV   decibels referenced to 1 volt

DC   direct current

HCPUA   heat capacity per unit area

MWNT   multi-walled carbon nanotube

NUWC   Naval Undersea Warfare Center

PAN   polyacrylonitrile

PZT   lead zirconate titanate

RMS   root mean squared

SPL   sound pressure level

TA   thermoacoustic

THIS PAGE INTENTIONALLY LEFT BLANK

I. INTRODUCTION

A. BACKGROUND

A thermoacoustic (TA) device is a device that uses rapid heat fluctuations to produce sound. Traditionally, sound is created by an oscillating surface that physically pushes and pulls on a fluid medium to create a pressure wave. In a thermophone, no motion is generated to actuate the particles in the medium. Alternating current (AC) is passed through a thin conductor, which causes it to rapidly heat and cool. This rapid temperature fluctuation is transferred to a thin layer of the fluid medium surrounding the conductor. These fluctuations in temperature lead to changes in the fluid pressure, which propagate away from the conductor as a sound wave [1].

Thermophones have a consistent sound output over a wide range of frequencies. This is because the sound source is not vibrating to produce the sound, and therefore does not have a resonant frequency like mechanical sound-generating equipment. The lack of moving parts in thermophones makes them predictable and thermophones have historically been used as precision sources of sound due to their consistency. Gold leaf or thin platinum sheets were often used as the conductors, which were then placed over a backplate to be used as a calibration tool [2] (Figure 1). These materials have been the most widely used for thermophones due to their relatively low heat capacity compared to other metals.
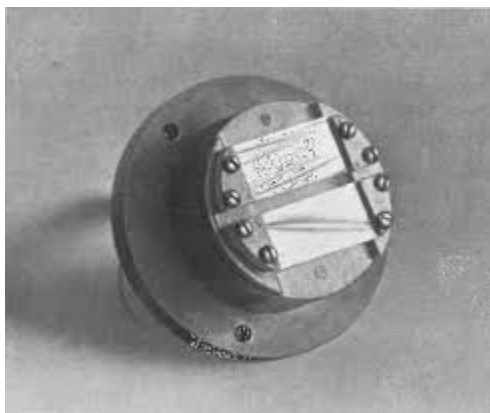
Figure 1.   An early thermophone attached to a backplate used for microphone calibration. Source: [2].

1

The disadvantage of thermophones is their inefficiency compared to conventional loudspeakers or traditional transducer materials such as PZT. Most of the input power is lost to heat that does not contribute to output root mean squared (RMS) pressure. In addition, thermophones are nonlinear transducers and therefore are not very suitable for reproducing a broadband signal such as music. Adding a direct current (DC) bias to the input AC signal can eliminate non-linear effects [1], but adding a bias decreases the efficiency of an already inefficient thermophone.

B.   APPLICATION OF CARBON NANOTUBE MATERIAL

In their original publication on thermophones, Arnold and Crandall noted three properties necessary for a TA material; it must be very thin, have a small heat capacity, and immediately conduct the temperature changes in its interior to its surface [1]. Arnold and Crandall used platinum sheets for their thermophones. These sheets had a heat capacity per unit area (HCPUA) of about 1 J/m^2 K. Carbon nanotube (CNT) sheets also possess properties suitable for use in thermophones. Current CNT sheets have a HCPUA of around 0.01 J/m^2 K, two orders of magnitude lower than that of platinum sheets and can possibly achieve even smaller values based on the thickness of the sheets [3].

The first exploration of CNTs for use in thermophones was performed by Lin et al. [4] at Tsingua University. Their thermophones were constructed by drawing a thin film from a CNT forest and placing them directly on electrodes (Figure 2). Many configurations, such as a cylindrical speaker and applying the CNT's to springs, were explored to showcase their flexibility. The results Lin et al. achieved were very promising. They reported sound pressure levels (SPL) similar to those of commercial loudspeakers and noted the versatility of CNTs for use on many surfaces and in many shapes.
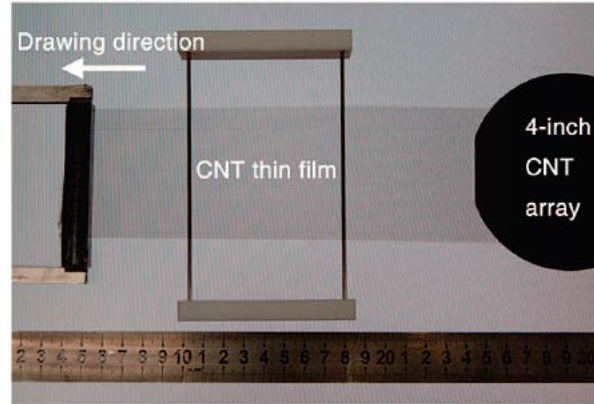
Figure 2.   Thin CNT film being extracted from a CNT forest
grown on a silicon wafer. Source: [4].

While CNT sheets have huge advantages for use in thermophones, there are still drawbacks that need to be overcome. The thin CNT sheets, used for thermophones, are very fragile and susceptible to damage by a small disturbance. The manufacturing process of drawing the CNT sheets from a wafer over the electrodes is tedious and requires careful use of special equipment. These disadvantages are in addition to the inefficiencies of TA devices in general and the nonlinearity of their sound reproduction. Follow-on research has focused on making the CNT TA devices more robust and efficient while maintaining the performance and versatility of the pure CNT sheets. A. E. Aliev at UT Dallas explored materials such as multiwalled carbon nanotube (MWNT) forests, graphene sponges, and electrospun polyacrylonitrile (PAN) sheets [5]. Those experiments show how different manufacturing techniques can be used to make CNT materials more suitable for TA applications.

C.   SCOPE OF THIS THESIS

This thesis aims to determine the TA performance of the Miralon® CNT sheets manufactured by Nanocomp and compare their performance to recently developed theory as well as other CNT-based TA materials. The focus will be on two sheets; one with area density of 10–15 g/m^2, and one with area density 20–30 g/m^2. Small samples of each sheet will be used to gauge how well they perform compared to each other. Sheets of varying shapes and sizes will be used to optimize the TA devices to match their impedance to that

3

of the specific circuit they are being actuated by. This thesis will also explore the frequency spectrum of the TA devices in order to determine the harmonics excited at different drive frequencies, as this has not been explored in depth in other papers relating to CNT TA devices. Finally, this thesis explores the linearity of TA response with respect to applied power.

II. THE PHYSICS OF THERMOPHONES

A. FUNDAMENTAL THEORY

The underlying physics of thermophones was first explored in detail in 1917 by Arnold and Crandall. They focused on actuating the thermophone in two ways; with a pure AC signal, and a DC biased signal. For a pure AC signal the heating effect can be described [1] as

$$P(t) = RI^2 \sin^2(\omega t),$$ (1)

where R is the resistance of the conductor, ω is the frequency of the drive signal, and P(t) is power delivered to the conductor. Using a simple trig identity, the equation can be rewritten as

$$P(t) = \frac{RI^2}{2}(1 - \cos(2\omega t)),$$ (2)

which shows the output frequency is double the input frequency [1]. Applying a DC bias that has a value several times the amplitude of the AC signal can eliminate this doubling of frequency. With a DC bias, P(t) [1] becomes

$$P(t) = R(I_0 + I\sin(\omega t))^2$$
$$= R(I_o^2 + \frac{I^2}{2}) + 2RI_0 I \sin(\omega t) - \frac{RI^2}{2}\cos(2\omega t),$$ (3)

which shows that for $I_o \gg I$, the cosine term becomes negligible and the double-frequency effect can be eliminated. Both equations 2 and 3 are proportional to the mean temperature of the conductor that determines the maximum acoustic output [1]. These equations show that a pure AC signal is best for producing a monotone signal. However, if the faithful reproduction of a signal is desired, such as for music, a DC bias needs to be superimposed on the AC signal.

For any TA heat source, the output root mean squared (RMS) pressure as a function of frequency [4] can be written as

$$P_{rms} = \left[\frac{\sqrt{\alpha}\rho_0}{2\sqrt{\pi T_0 C_h}} \right] \cdot \frac{\sqrt{f}\,P_h}{r}, \tag{4}$$

where α is the thermal diffusivity of the surrounding gas, ρ_o is the gas density, T_o is the temperature of the gas, C_h is the heat capacity of the heater (per unit area), P_o is the power applied, and r is the distance from the heater The most important thing to note is that the heat capacity is in the denominator, meaning a lower heat capacity is required to increase output RMS pressure.

B.   DEVELOPMENTS AND CORRECTIONS FOR CNT THERMOPHONES

The theory developed above was tested against the 700 nm platinum sheets used by Arnold and Crandall. Since CNTs have a much lower heat capacity than any previous TA material, a correction was developed to more accurately describe CNT thermophones specifically. Lin et al noted that Equation 4 does not fully describe the rms pressures generated by their CNT thermophones. By considering the rate of heat lost per unit area per unit temperature rise (β_0) and the heat exchange between the CNT film and the surrounding gas, they were able to derive a correction factor that more accurately describes the rms pressure generated by a CNT TA device [4] as

$$P_{rms} = \left[\frac{\sqrt{\alpha}\rho_0}{2\sqrt{\pi T_0 C_h}} \right] \cdot \frac{\sqrt{f}\,P_h}{r} \cdot \frac{\dfrac{f}{f_1}}{\sqrt{(1+\sqrt{\dfrac{f}{f_1}})^2 + (\dfrac{f}{f_2}+\sqrt{\dfrac{f}{f_1}})^2}}, \tag{5}$$

where $f_1 = (\alpha\beta_0{}^2)/(\pi\kappa^2)$ and $f_2 = (\beta_0)/(\pi C_s)$, κ is the thermal conductivity of the gas, and C_s is the heat capacity of the surrounding medium. For any frequency $f \gg \kappa^2/\pi\alpha C_h{}^2$, Equation 5 simplifies to Equation 4. Using the HCPUA of a thin platinum sheet, that frequency is 2.45 Hz. For a thin CNT sheet, that frequency is 1.65 MHz. Virtually no applications of acoustics use frequencies close to 1.65 MHz, so Equation 5 is the best theoretical prediction of a CNT thermophone output. Figure 3 is a comparison of equations 4 (blue) and 5 (orange). At the heat capacity of a platinum sheet (1 J/m^2 K), both equations predict the same sound pressure level (SPL). However, Equation 4 overestimates the SPL

of TA material that has the ultra-low heat capacity of a CNT sheet, which is denoted by the leftmost vertical line.
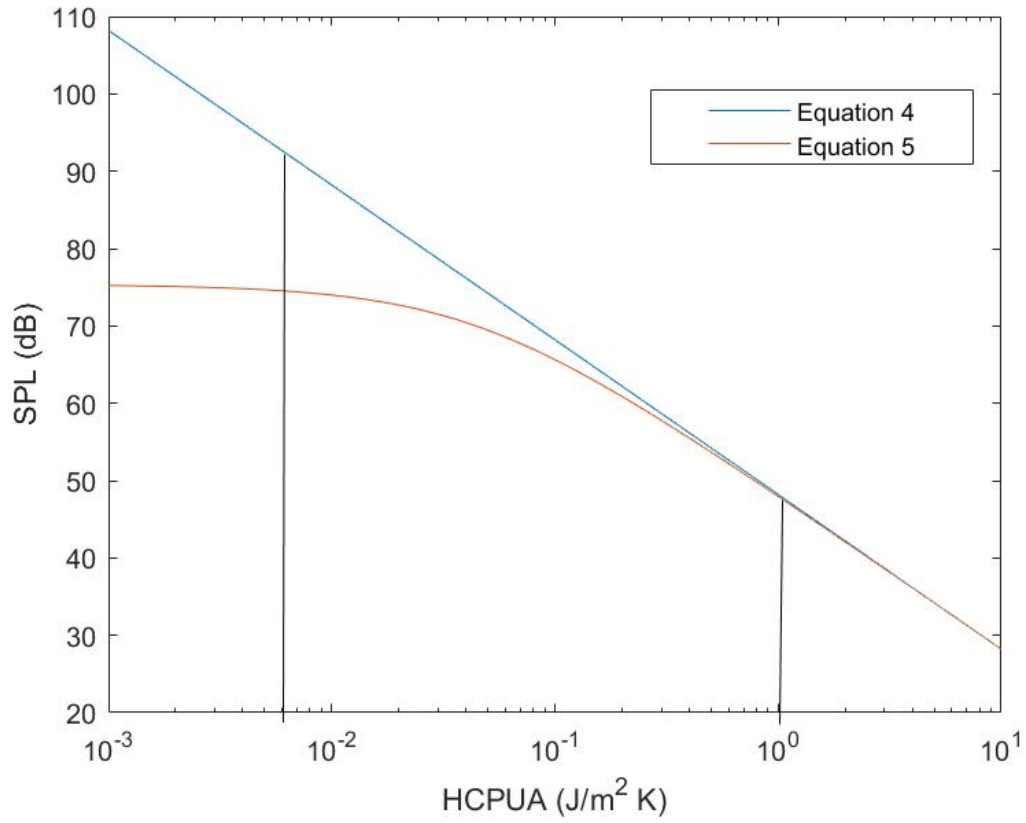

Figure 3.   Plot showing the predicted SPL of a TA device using theory developed by Arnold and Crandall [1] (blue), and Lin et al. [4] (orange). This plot assumes 1 Watt of applied power at a frequency of 10 kHz.

THIS PAGE INTENTIONALLY LEFT BLANK

III. FABRICATION AND EXPERIMENTAL SETUP

A. MAKING THE TA DEVICES

The creation of the TA devices was remarkably simple and required no specialized equipment. The support structure consists of insulated copper wires threaded through a plastic holder. The wires are stripped in order to expose the copper for application of the CNT sheets. H20E EPO-TEK® silver conductive epoxy is used to adhere the CNT sheets to the copper wire (Figure 4). This epoxy is two parts mixed in a 1 to 1 ratio and then smeared onto the copper wire. The CNT sheets are cut to an appropriate size using a pair of scissors, then applied to the copper. The epoxy is applied to one exposed copper wire and one end of the CNT sheet is wrapped around the exposed copper. Then the sheet is laid across and wrapped around the other copper wire. A period of 24 hours is required for the epoxy to completely dry.
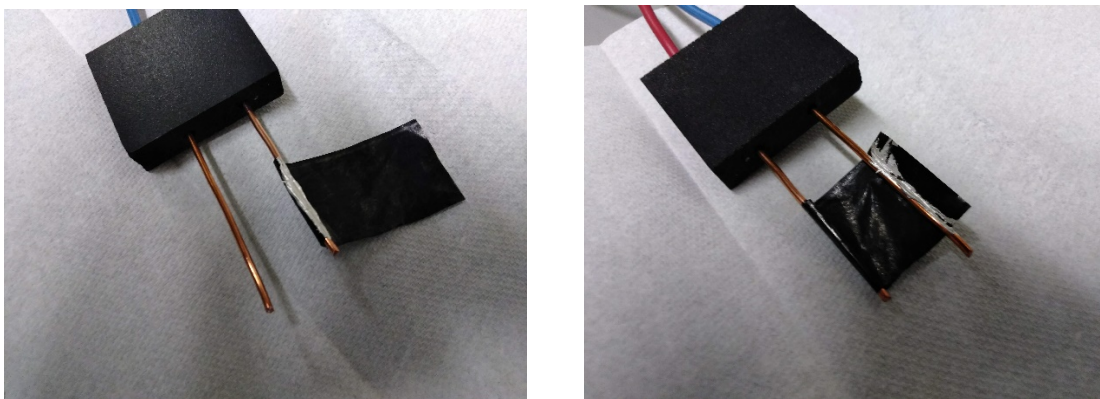
Figure 4.   CNT sheet being wrapped around copper wire with conductive paste applied.

B.   EXPERIMENTAL SETUP AND METHODOLOGY

The design of the experiment can be broken up into two parts; varying the parameters of the input signal through the TA device and recording the output of the TA device.

1.   Input Signal

The input signal is a pure AC sinusoidal wave supplied by a function generator and run through an amplifier. Metal clips are attached to the exposed end of the copper wire to complete the circuit (Figure 5) The two main parameters of interest are the input frequency and the power applied to the CNT sheet. While varying frequency, the RMS voltage of the AC signal remains constant.

Figure 5.   Signal input setup with function generator connected to amplifier.

The output RMS voltage of the function generator was varied from 1.00 Vrms to 3.50 Vrms to vary the power applied to the TA devices at a constant frequency. A frequency of 3 kHz was chosen for the sake of comparison to m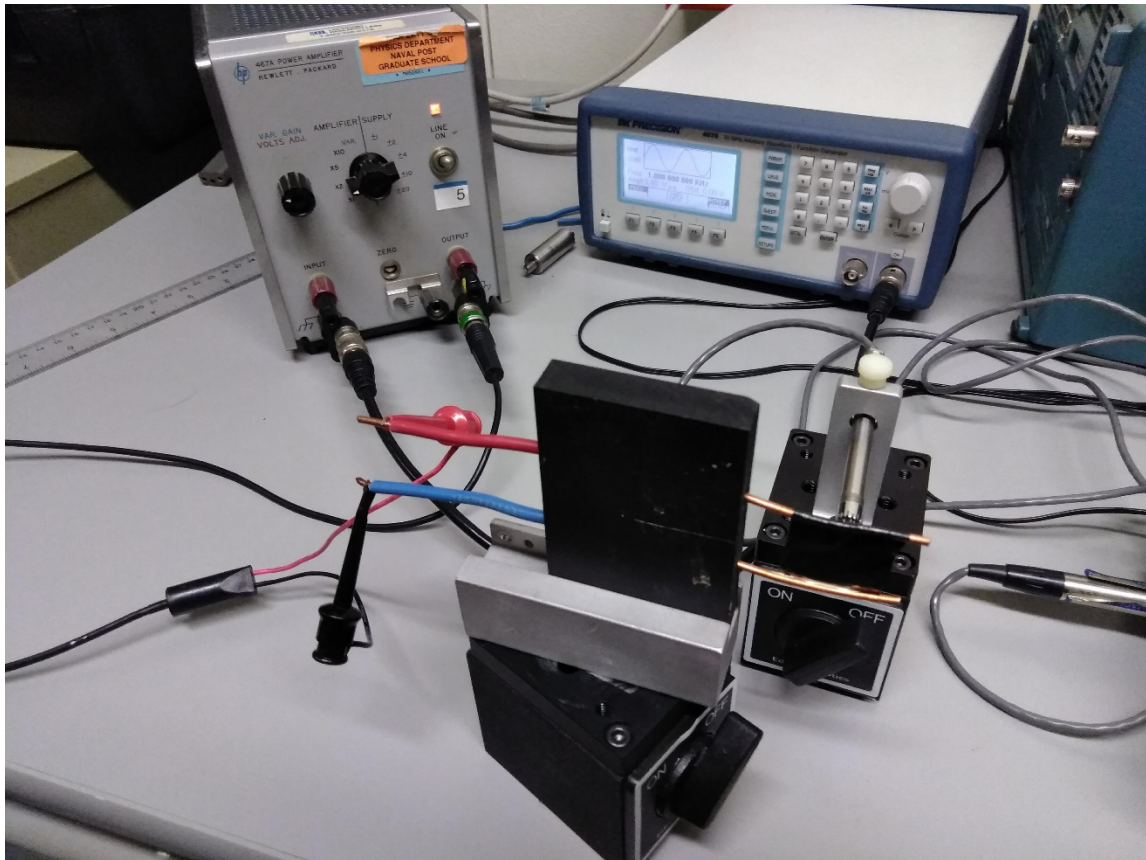aterials in the paper by A. E. Aliev [5]. Power was calculated by measuring voltage and current across the CNT sheet with a Fluke multimeter.

2. Thermophone Output

To measure the output RMS pressure of the TA device, a microphone is held a set distance away and connected to a lock-in amplifier. Two microphones were used. The first was a Larson Davis 1/4 inch microphone for frequencies from 500 Hz to 20 kHz (Figure 6). This microphone has a pre-amp with adjustable gain (Figure 7). The second microphone used was a B&K 1/8 inch microphone for measuring frequencies up to 100 kHz. This microphone does not have an adjustable pre-amp (see the Appendix for microphone specifications). Both microphones were placed 1 cm away from the CNT sheets for measurements and were connected to a Stanford Research Systems SR850 lock-in amplifier. A lock in amplifier is needed to focus on the second harmonic of the drive frequency, which is predicted to have the strongest signal. Ambient air temperature was monitored using a mercury thermometer and varied from 23 to 25 ℃. A FLIR Systems i3 camera was used to record surface temperature of the CNT sheets during testing. Temperature was used as an indicator for power being delivered to the CNT sheet. A higher surface temperature indicates more power is being delivered to the CNT sheet and that power is being dissipated as heat. However, a higher temperature does not necessarily mean a higher output RMS pressure since some of that could be wasted heat.
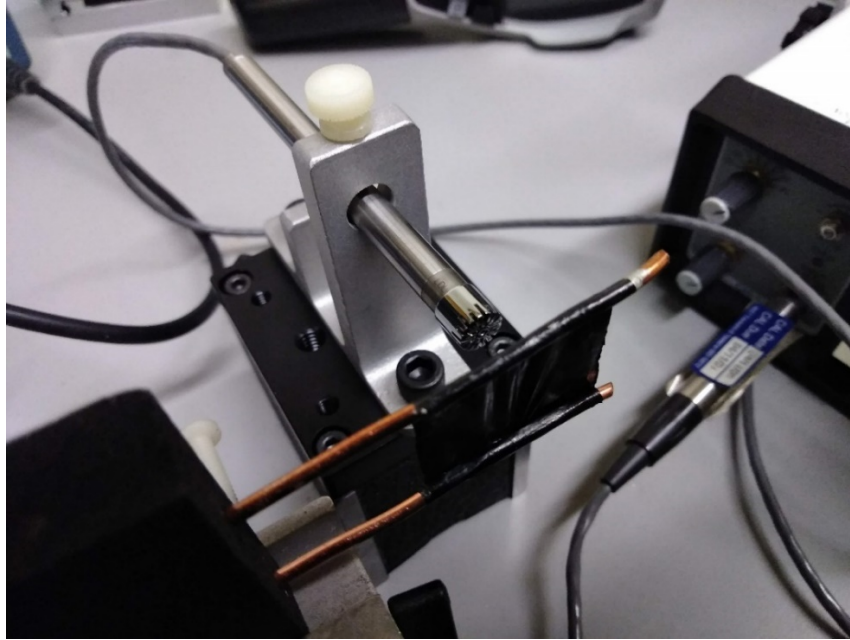
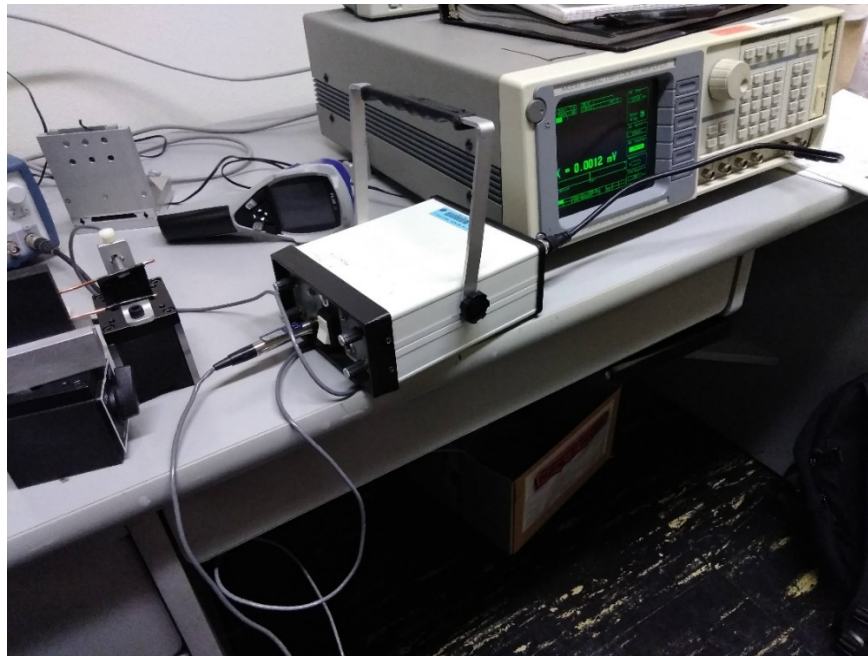Figure 6.   Quarter-inch microphone placed to record thermophone output.

Figure 7.   Larson Davis pre-amp connected to lock-in amplifier.

C.   IMPEDANCE MATCHING

The goal of impedance-matching is to deliver power to a load at the maximum possible efficiency. This is done by matching the impedance of the load (sheet) to the impedance of the source (amplifier). For the setup shown in Figure 5, this would mean matching the impedance of the function generator and amplifier to the impedance of the CNT sheet. Figure 8 is a simplified diagram of the setup shown in Figure 5. In most cases, the output impedance of an amplifier is real, meaning that it can be considered as a pure resistor. This means that the load should also be purely resistive [6]. The challenge is that CNT sheets are not purely resistive at all frequencies. Research at Michigan Tech showed that the CNT sheets used by them were purely resistive until about 10 kHz (Figure 9). A similar behavior for the Miralon® sheets can be expected. Therefore, the most efficient response of the CNT thermophones tested will most likely be at low frequencies. Impedance matching can be achieved over a wide range of frequencies by placing an impedance matching circuit or device between the source and the load [7]. Such a device is not used in the experiments described above. Another solution is to increase the power of the drive such that the impedance mismatch is no longer a factor [6], however this is not possible with the setup described.
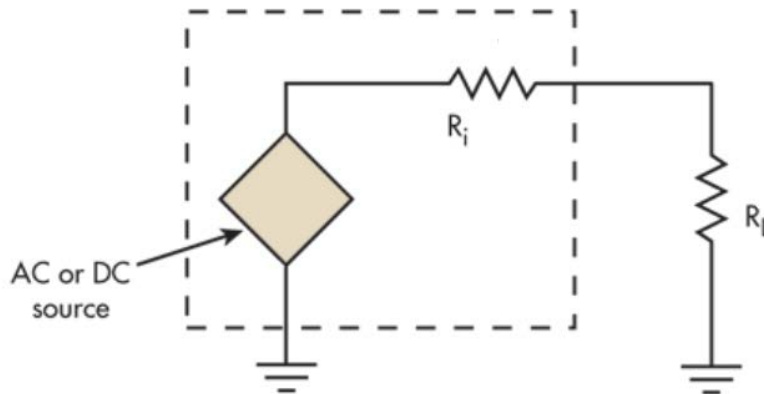

Figure 8.   Simple circuit diagram of setup shown in Figure 5. The most efficient power delivery occurs when Ri = RL. Source: [7].
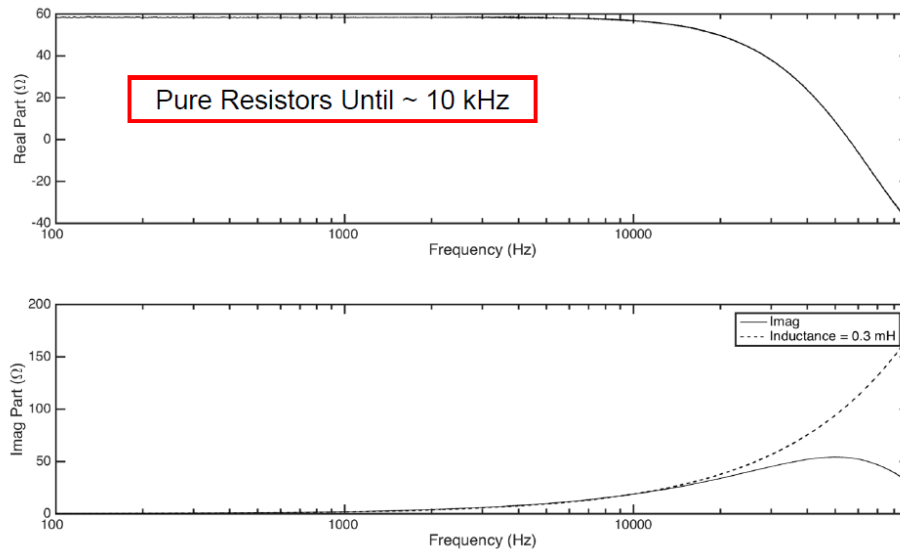
13

Figure 9.   Plots of the real part (resistance) and imaginary part (reactance) of the TA device used in Michigan Tech's experiments. Source: [3].

IV. RESULTS AND DISCUSSION

A. INITIAL TESTING

The first round of experiments focused on comparing the 10-15 grams per square meter (gsm) sheet and the 20–30 gsm sheet, which will from this point on be referred to as the *low-density sheet* and *high-density sheet*, respectively (see the Appendix for material properties). The low-density sheet has dimensions of 2.3 x 2.4 cm, a resistance of 2.0 ohms, and a mass between 0.006 grams and 0.008 grams. The high-density sheet has dimensions of 2.5 x 3.0 cm, a resistance of 0.7 ohms, and a mass between 0.015 grams and 0.023 grams. When recording the RMS pressure, values for the first and second harmonic were measured. Whichever value was higher was used in the plots.

1. Low-Density Sheet

At drive frequencies below about 10 kHz, the response of the low-density sheet closely follows the theory of Equation 5. Equation 4 overestimates the RMS pressure due to the low heat capacity of the Miralon® sheet. As the frequency gets closer to 20 kHz, the response of the sheet drops well below the theoretical prediction (Figure 10). This trend was also observed in a paper by A. E. Aliev, M.D Lima, S. Fang, and R. H. Baughman published in Nano Letters and was attributed to the increased difficulty of dissipating heat at higher frequencies [8]. The decline in output could also be attributed to the impedance mismatch limiting the power delivered to the TA device. For calculating the theoretical lines, equations 4 and 5 used 0.05 Watts for the power applied, 0.01 meters for the distance from the CNT sheet, and a HCPUA of 0.05 Joules per square meter. In Figure 11, data from the 1/8 inch B&K microphone is included to show higher frequency measurements. These measurements are far more sporadic than the measurements at lower frequencies with the 1/4 inch Larson Davis microphone.
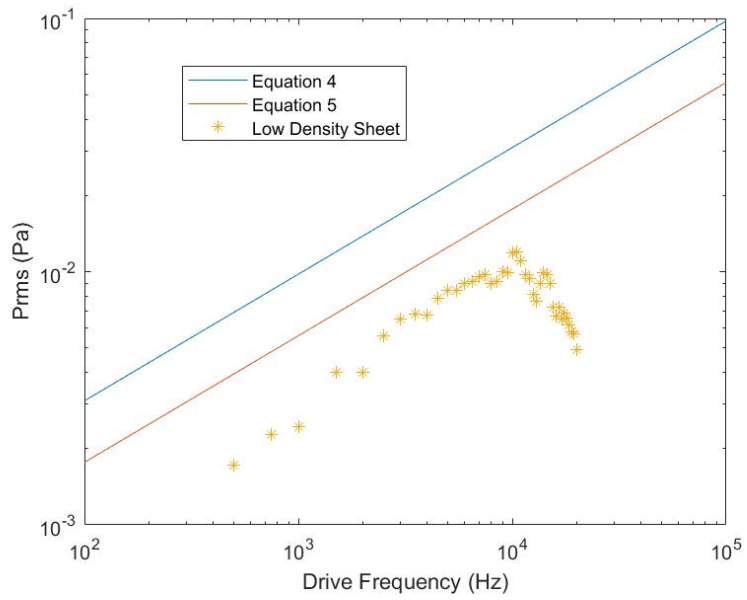
Figure 10.   Low frequency response of the low-density sheet.
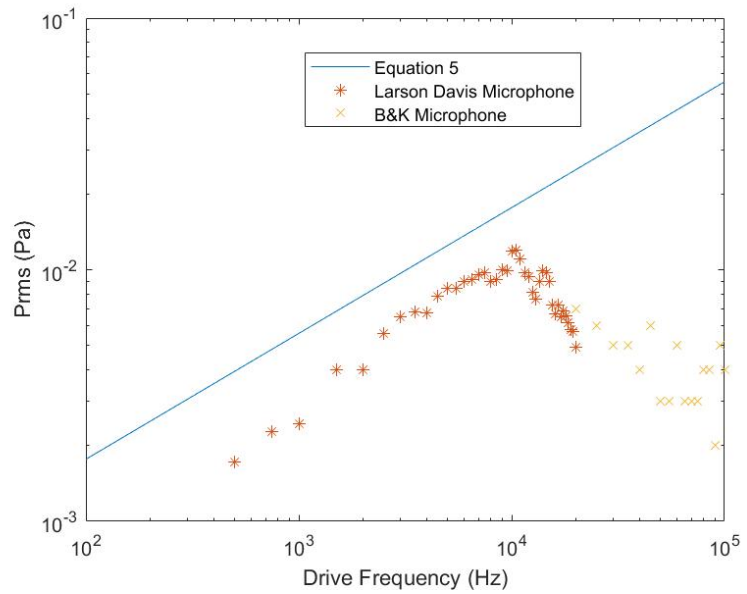

Figure 11.   Frequency response of low-density sheet with high
frequency measurements.

In Figure 12, data from the 1/8-inch B&K microphone is included to show higher frequency measurements. These measurements are far more sporadic than the measurements at lower frequencies with the 1/4-inch Larson Davis microphone.

Figure 12 focuses on how the RMS pressure output varies with applied power. The drive frequency used was 3 kHz. The RMS voltage supplied was varied from 1.0 Vrms to 3.5 Vrms and power was calculated by multiplying voltage and current across the CNT sheet. RMS pressure varies widely with applied power for the low-density sheet and does not appear to follow the trend of the theoretical curve. Temperature has a similar variation with power as shown in Figure 13. There does not appear to be any strict pattern. When RMS pressure is plotted against temperature, a rough linear relation is present (Figure 14). When maximum power was achieved, which was about 0.05 watts, the surface temperature of the low-density sheet reached 99 °C (Figure 15).
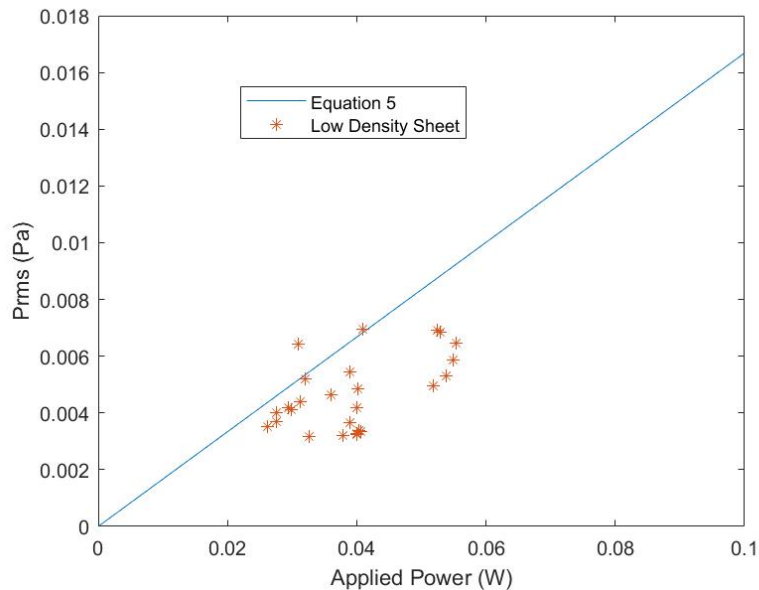

Figure 12.   RMS pressure with varying power at a 1.5 kHz compared
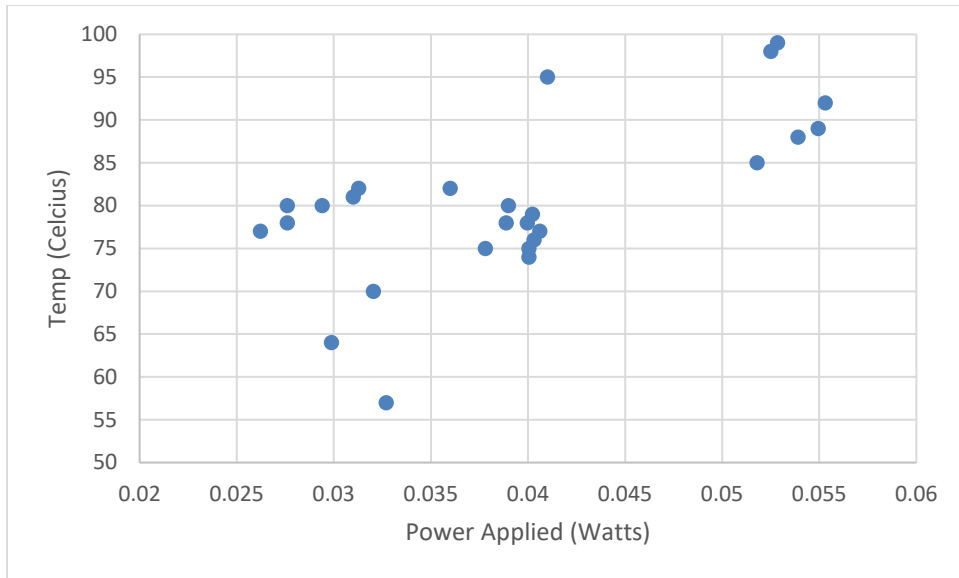to Equation 5 prediction.

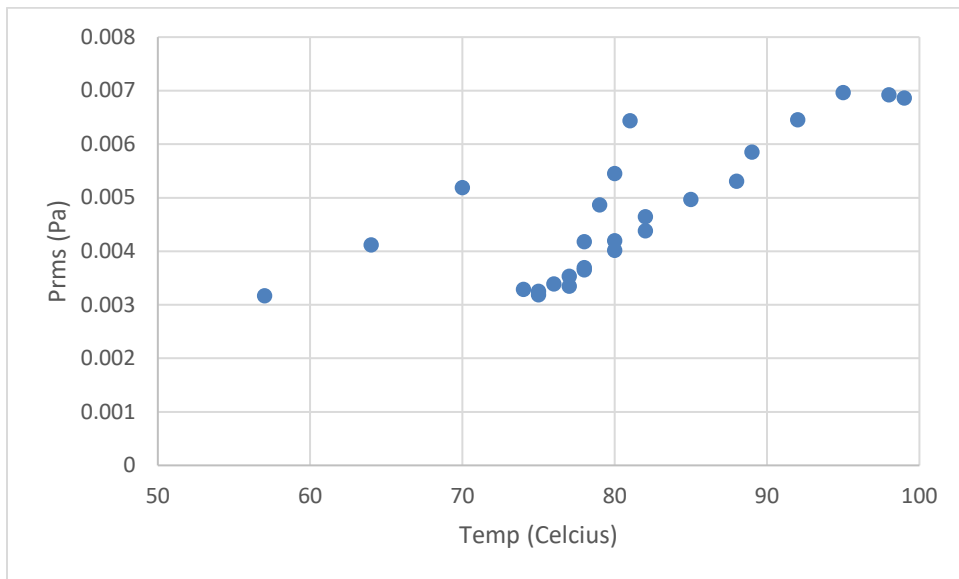Figure 13.   Temperature variation with applied power.

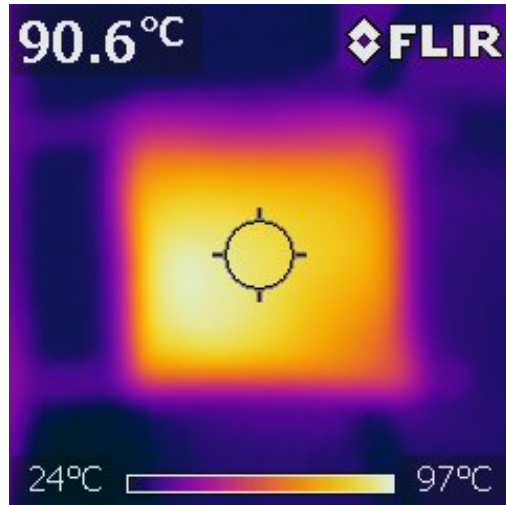Figure 14.   RMS pressure variation with surface temperature.

18

Figure 15.   Thermal image of the low-density sheet at maximum applied power.

2.   High-Density Sheet

Like the low-density sheet, the high-density sheet followed the theoretical prediction of Equation 5 until about 10 kHz. Again, Equation 4 predicts a higher RMS pressure output than Equation 5. However, the two lines are closer together since Figure 16 uses a HCPUA of 0.1 Joules per square meter to plot the theoretical lines. As heat capacity increases, Equation 4 becomes a better approximation for Equation 5. The high-density sheet has a maximum RMS pressure output of about 0.004 Pascals, which is much lower than the 0.012 Pascal maximum of the low-density sheet. The lower RMS pressure output can be attributed to the higher thermal mass of the high-density sheet. It takes longer for the high-density sheet to heat and cool compared to the low-density sheet. As a result, the high-density sheet experiences a lower maximum temperature, which correlates to a lower RMS pressure (Figure 19).

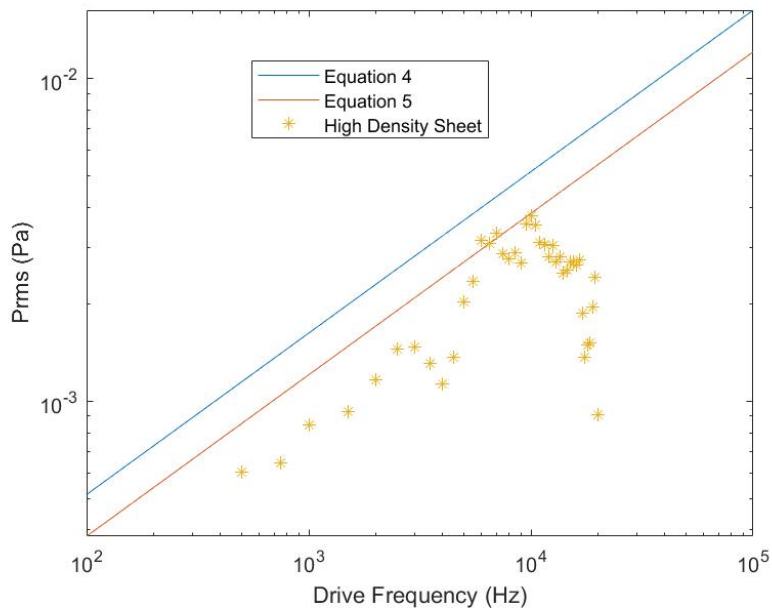Figure 16.   Low frequency response of the high-density sheet.
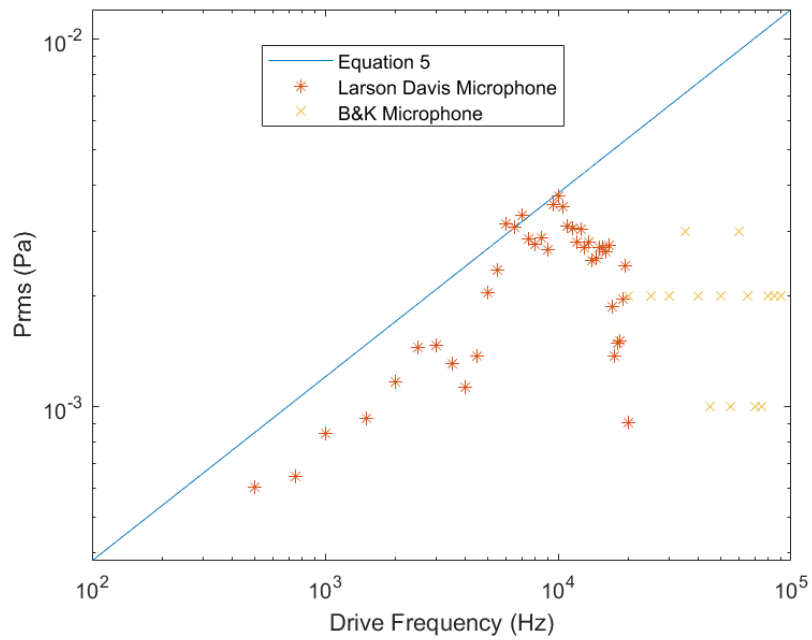

Figure 17.   Frequency response of the high-density sheet with high
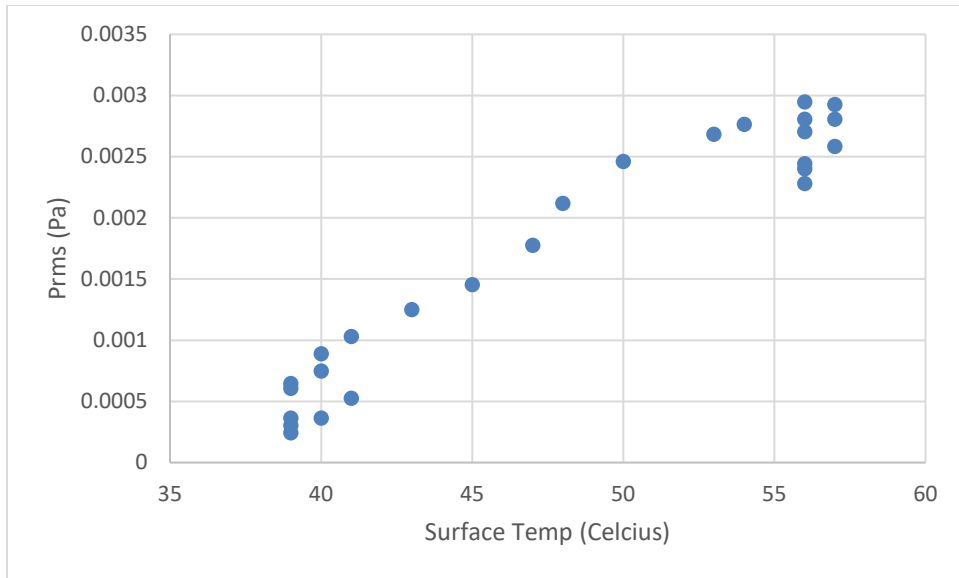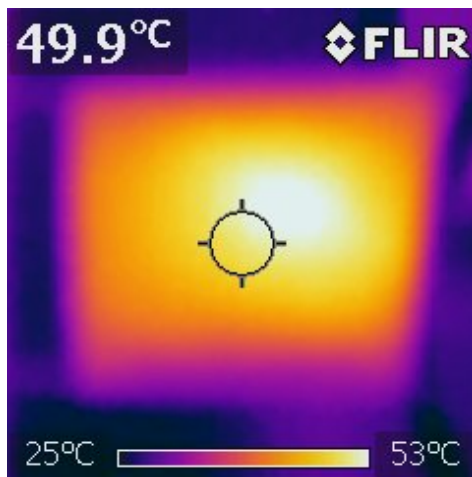frequency measurements.

Figure 18.   RMS pressure variation with surface temperature of the high-density sheet.

Note the maximum temperature is about half that of the low-density sheet.

Figure 19.   Thermal image of the high-density sheet at maximum applied power.

B.   OPTIMIZING THE THERMOPHONE

1.   Narrow Strip

One factor limiting the performance of the TA devices tested is the low resistance of the sheets. This low resistance limits the power that can be delivered to the CNT sheets. By increasing the resistance, more power can be delivered to the CNT sheet. One way to increase the resistance is to change the geometry of the CNT sheet. Instead of placing a square across the copper, a long and thin rectangle is used. In this configuration, which will be referred to as the *narrow strip* the current has to travel a longer distance and has less paths to take from one copper to the other (Figure 20). This configuration has a resistance of 4.5 Ohms compared to a resistance of 2.0 Ohms in the original configuration with the low-density sheet. With dimensions of 8 cm x 1.4 cm, the CNT sheet has a mass between 0.0112 grams and 0.0168 grams.
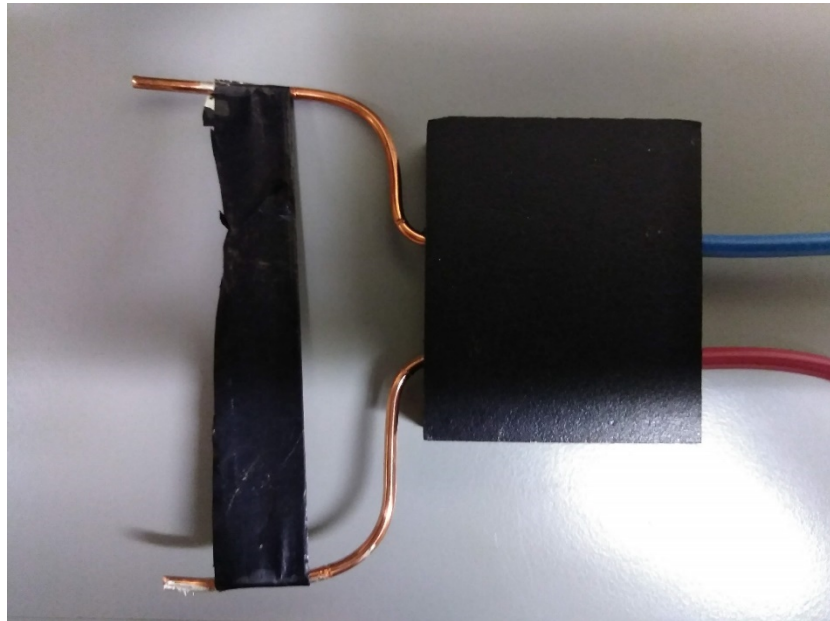

Figure 20.   Low-density sheet in the narrow strip configuration.

Using the new narrow strip configuration, the RMS pressure output by the low mass CNT sheet is increased at frequencies between 500 Hz and 2 kHz (Figure 21). The drop in RMS pressure at 2 kHz can be attributed to the increases mass of this narrow strip. This

narrow strip is about double the mass of the previous low-density sheet that was a square. That sheet experienced an RMS pressure decrease at about 10 kHz. As a result of the increased mass, this narrow strip takes longer to heat and cool. This means that the narrow strip cannot dissipate heat quickly enough beyond 2 kHz to keep increasing its RMS pressure output.

Despite the reduced RMS pressure above 2 kHz, more power can be delivered the narrow strip than can be delivered to the previous CNT sheets at a drive frequency of 1.5 kHz (Figure 22). The narrow strip clearly follows the theory predicted by Equation 5, albeit the actual RMS pressure is consistently below the theoretical value. This is in stark contrast to the previous configurations where there was no trend in RMS pressure when plotted against applied power. In addition, the relations between power, surface temperature, and RMS pressure are clearly linear and have no outliers (Figures 23 and 24). All these trends are likely the result of the increased resistance of the narrow strip allowing power to be applied more efficiently to the CNT sheet.
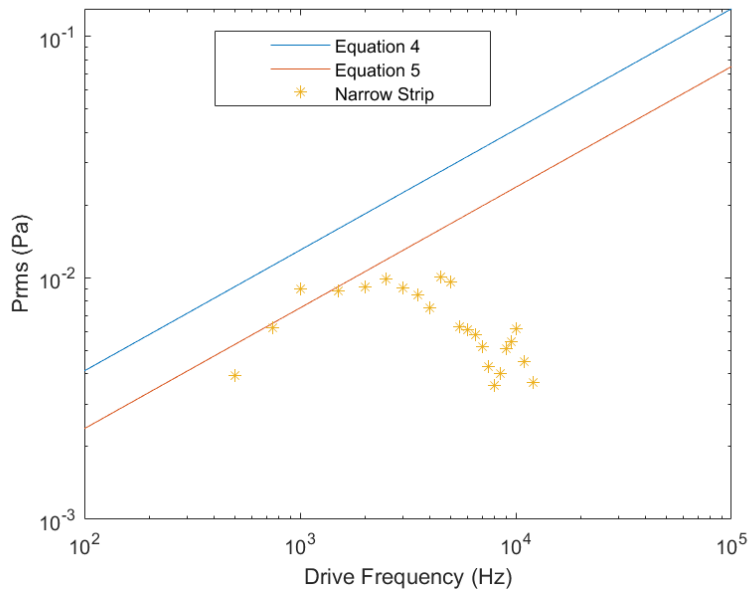
Figure 21.   Frequency response of the narrow strip recorded with the
1/4 inch Larson Davis microphone.
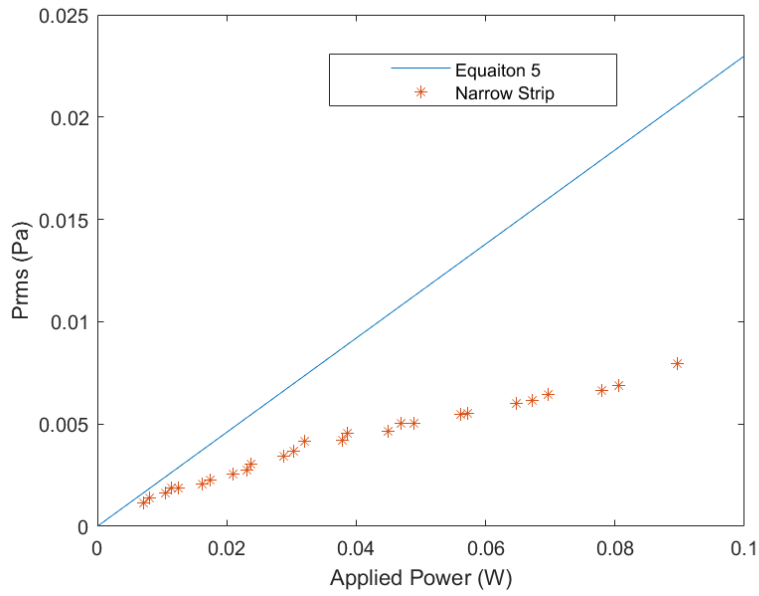
Figure 22.   RMS pressure variation with applied power compared to
Equation 5.
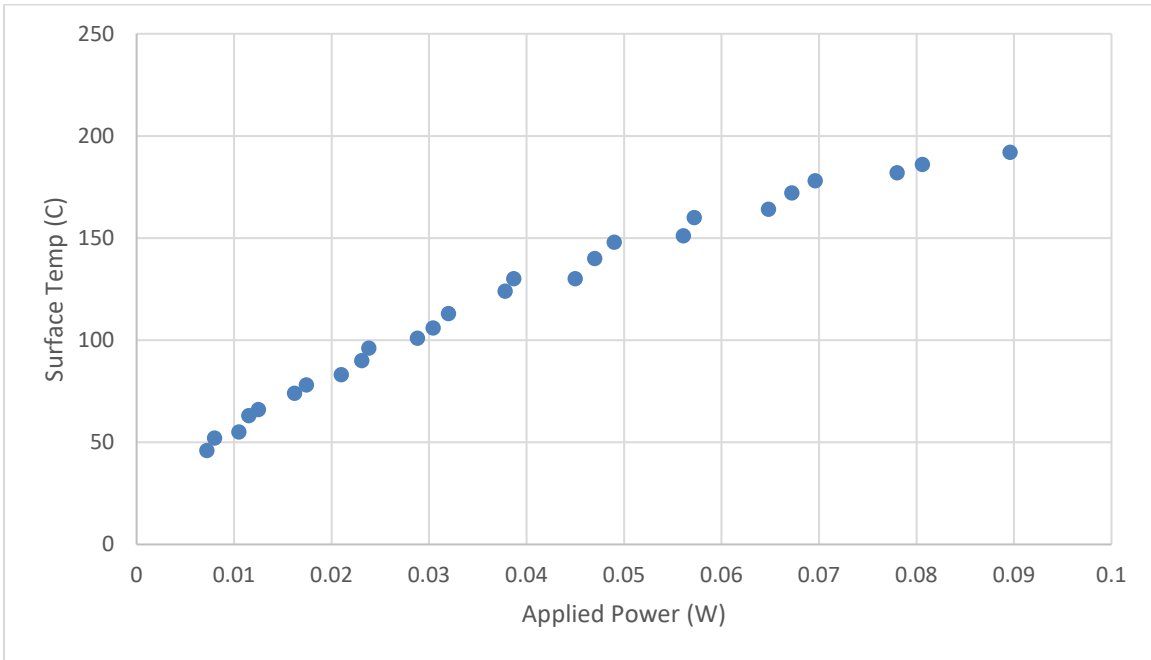
Figure 23.   Temperature variation with applied power.

24
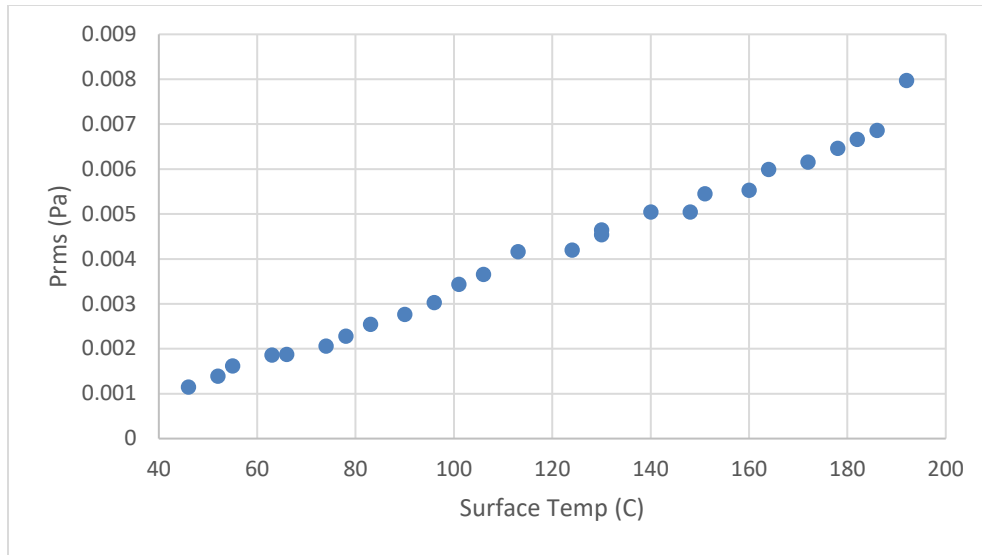
Figure 24.   RMS pressure variation with surface temperature.

The narrow strip experiences a higher maximum surface temperature than the previous samples, which is indicative of the higher power being delivered (Figure 25).

Figure 25.   Thermal image of the narrow strip at maximum applied power.

The last figure in this section (Figure 26) is a comparison of the RMS pressure of this narrow strip compared to two other CNT based materials tested by A. E. Aliev;

multiwalled carbon nanotube (MWNT) forest and electrospun polyacrylonitrile (PAN) sheets [5]. Aliev's data was normalized based on the distance to microphone, 3 cm in this case. That data is plotted in Figure 26 with the raw data from the narrow strip. While all three m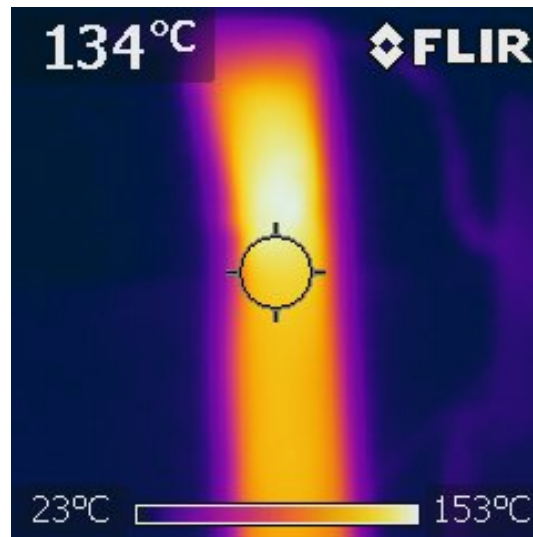aterials output similar RMS pressures below 2 kHz, the MWNT and PAN materials continue to output higher RMS pressures after the narrow strip begins to decrease its RMS pressure output. Again, the mass of the narrow strip combined with the fact that the narrow strip is not impedance matched in its circuit reduces the frequency at which its RMS pressure output is maximized.
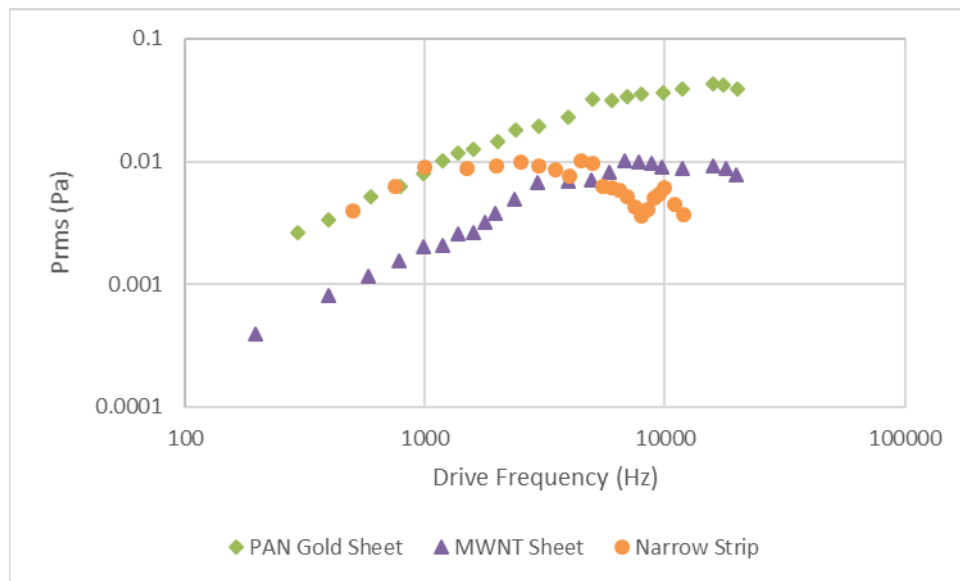
Figure 26.   Frequency sweep comparison of the narrow strip to two materials tested in the paper by A. E. Aliev. Data source: [5].

2.   Small Narrow Strip

Based on the previous narrow strip, the best configuration to maximize RMS pressure is a strip of the same proportions but lower mass. That configuration, referred to as the *small narrow strip*, is shown in Figure 27. It has dimensions of 4.0 cm x 0.5 cm and a mass between 0.002 grams and 0.003 grams. The resistance of the strip is 10 Ohms
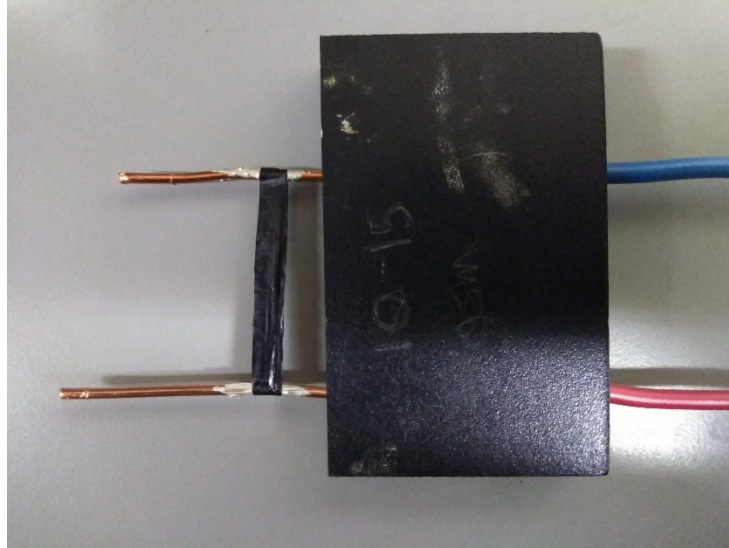
Figure 27.   Low mass narrow strip configuration.

The low mass narrow strip follows the theoretical line of Equation 5 up to about 20 kHz (Figure 28). This performance is much better than the narrow strip since the mass has been reduced by an order of magnitude. There is a drop in RMS pressure between 6 kHz and 10 kHz. This drop is most likely due to an impedance mismatch causing a reduction in power being delivered to the CNT sheet. Figure 29 shows RMS pressure variation with power and looks very similar to Figure 22. The high resistance coupled with the low mass allows power to be delivered more efficiently when compared to the original square configuration of the low-density sheet (see Figure 12). When compared to the MWNT sheet and PAN sheet tested by Ali Aliev [5], the low mass narrow strip has the highest RMS pressure output at low power (Figure 30). The theoretical line in Figure 30 assumes a HCPUA of 0.05 J/m^2. Aliev was able to apply much more power to the MWNT and PAN sheets. It is expected that given more applied power, the RMS pressure generated by the low mass narrow strip would deviate from the theoretical curve in a similar way to the MWNT sheet and PAN sheet.

Figure 28.   Frequency response of the low mass narrow strip recorded
with the 1/4 inch Larson Davis microphone.
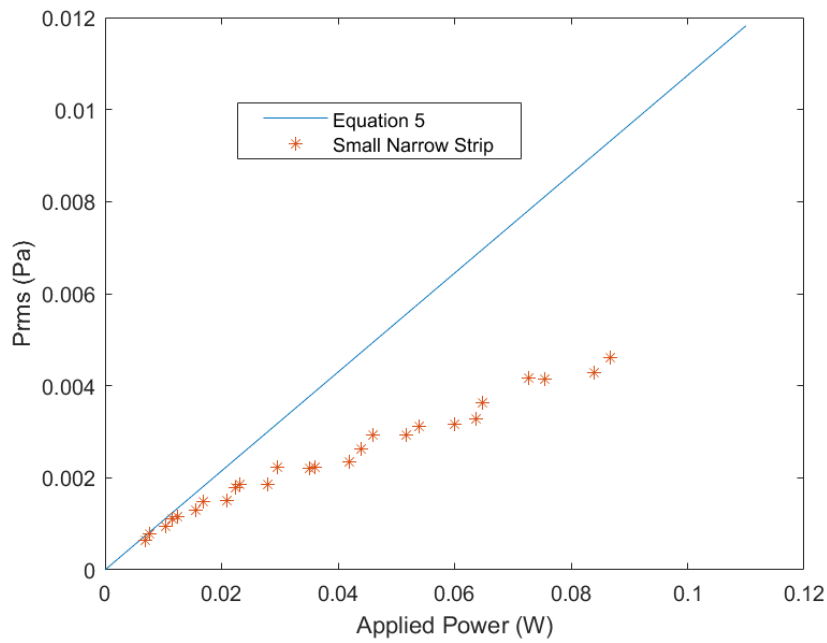
Figure 29.   RMS pressure variation with applied power at 1.5 kHz
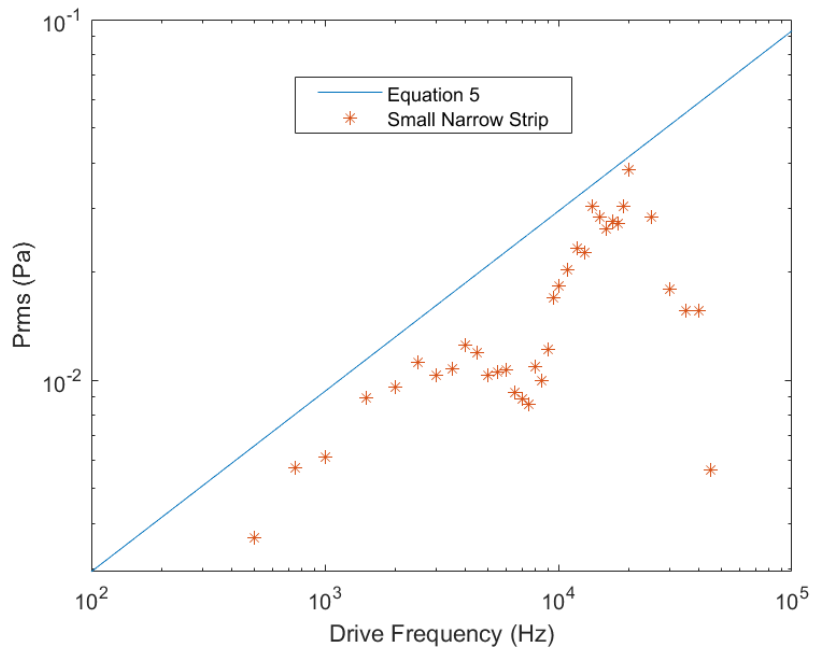drive. Recorded at 3 kHz.
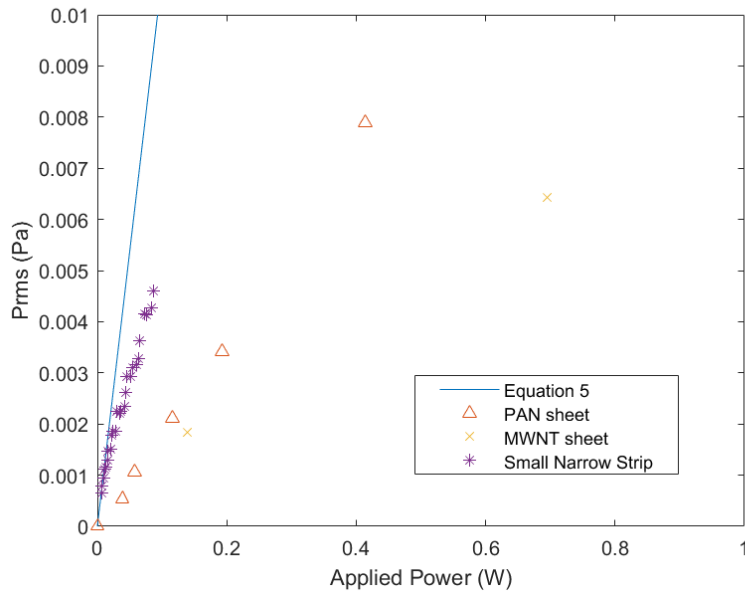
Figure 30.   Comparison of RMS pressure variation with power to two
materials tested in the paper by A. E. Aliev. Data source: [5].

Given the low mass and high resistance of the small narrow strip (more closely matching that of the amplifier output), it's no surprise that this configuration experiences the highest surface temperature at maximum applied power out of all the configurations (Figure 31). The relation between applied power and surface temperature is linear, as is the relation between temperature and RMS pressure (Figures 32 and 33).

Figure 31.   Thermal image of low mass narrow strip at maximum
applied power.

29

Figure 32. Temperature variation with applied power.

Figure 33. RMS pressure variation with surface temperature.

Comparing the small narrow strip to the MWNT sheet and PAN sheet, it is clear that the RMS pressure output at higher frequencies is much improved over the narrow strip (Figure 34).
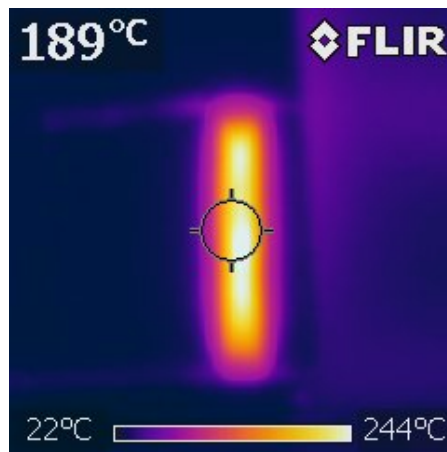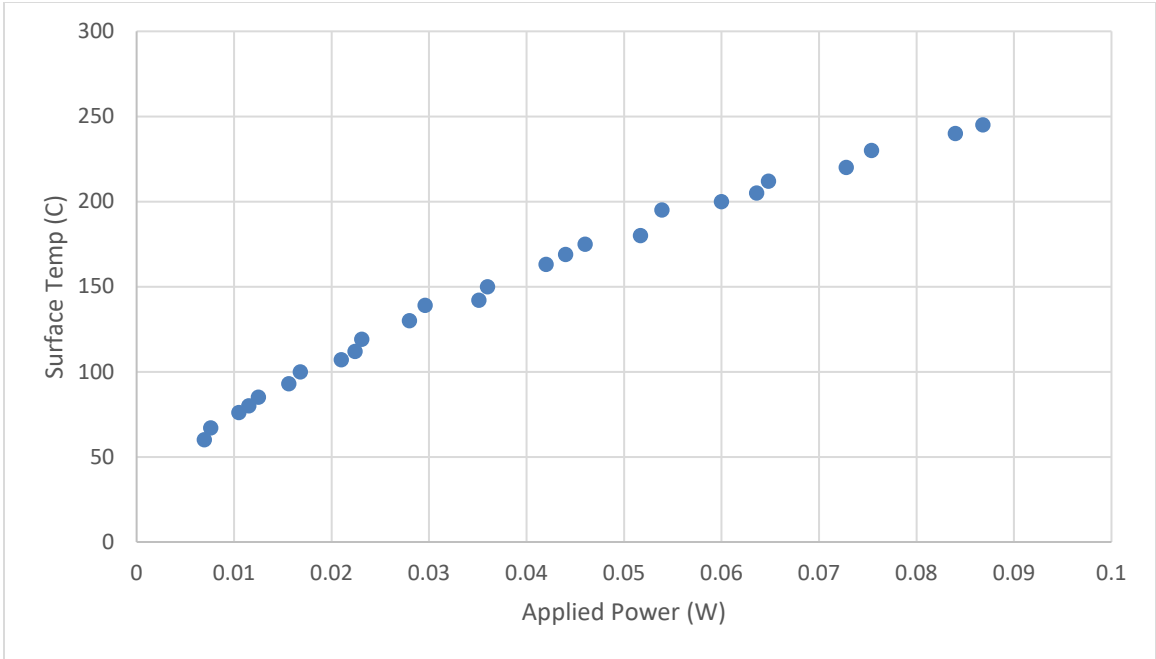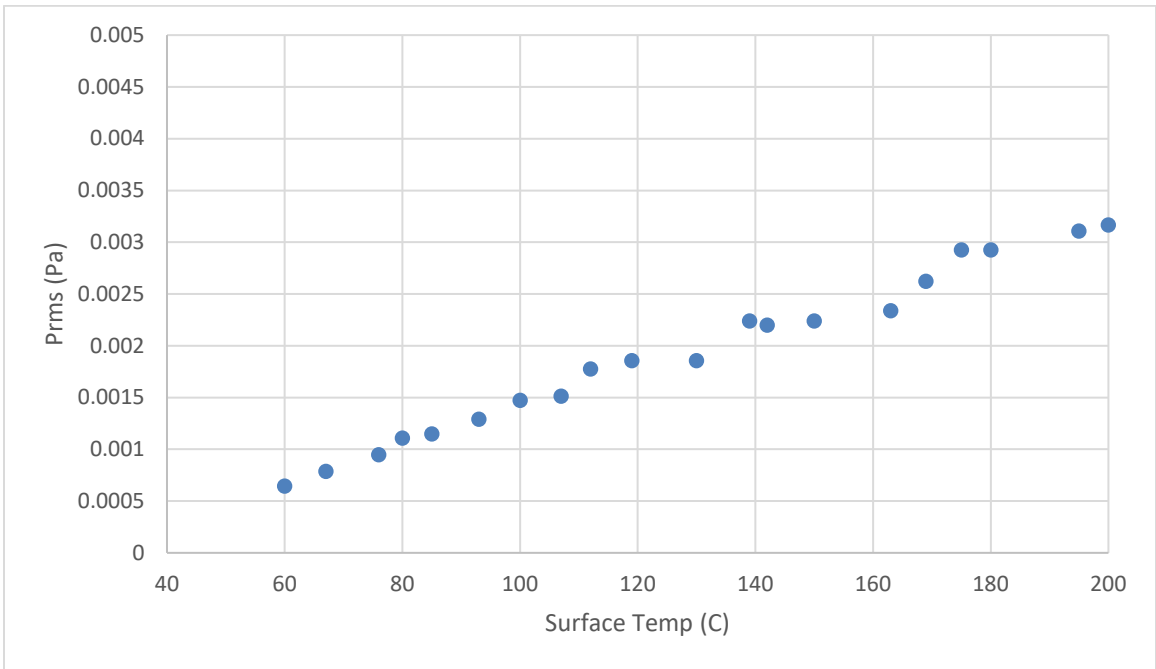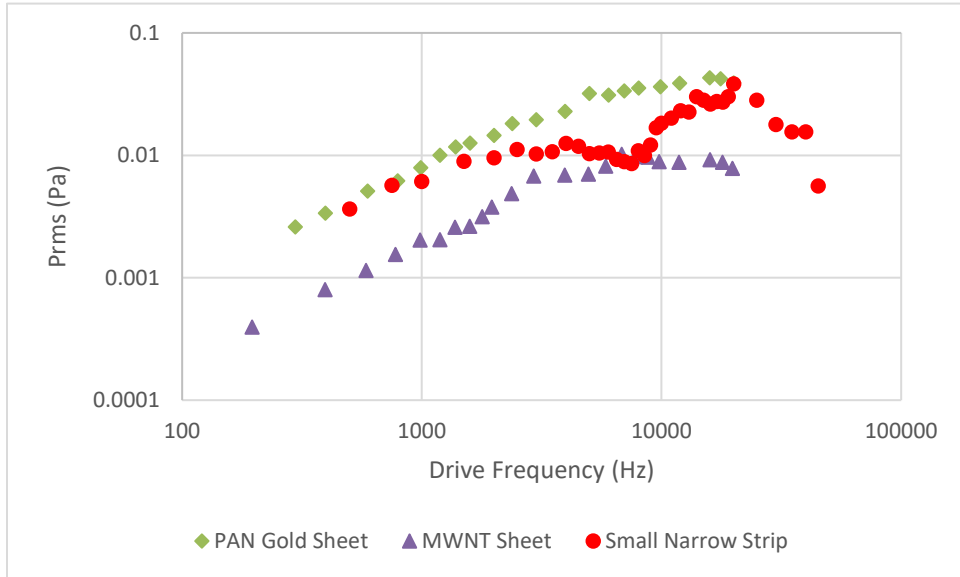

Figure 34.   Frequency sweep comparison of the low mass narrow strip
to two materials tested in the paper by A. E. Aliev.
Data source: [5].

C.   EXPLORATION OF THE FREQUENCY SPECTRUM

When measuring the RMS pressure of the thermophones, both the first and second harmonics were measured, and the highest response was recorded. According to the double frequency effect, a thermophone will produce a tone at twice the frequency of the drive. However, when measuring the RMS pressure output by the thermophones, the second harmonic was not always the strongest signal. Looking at the frequency spectrum of the thermophones reveals the relative strength of each harmonic given a certain drive frequency. Figure 35 shows the spectra of the low-density sheet. For a 2 kHz drive frequency, the second harmonic is approximately equal in strength to first harmonic with the third through fifth harmonics well below the level of the first and second. When driven at 5 kHz, the second harmonic is clearly stronger than the first as the double frequency

31

effect would predict. At driving frequencies of 10 kHz and above, the second harmonic is at or below the level of the first harmonic, contradicting the double-frequency effect.
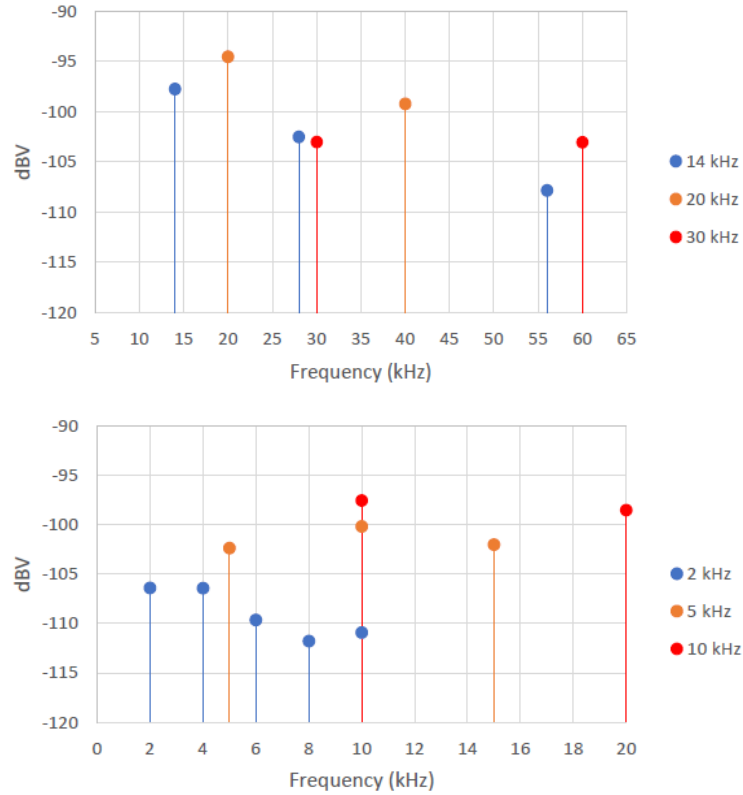
Figure 35.   Frequency spectrum of the low-density sheet.

Figure 36 shows the frequency spectra for the high-density sheet. Compared to the low-density sheet, the second harmonic is clearly stronger than the first at a drive frequency of 2 kHz. In addition, the gap between the first and second harmonic is much larger for the high-density sheet. At 2 kHz, the second harmonic is about 5 dBV greater than the first, compared to no difference with the low-density sheet. At 5 kHz, the second harmonic is about 6 dBV greater compared to 3 dBV for the low-density sheet.

32
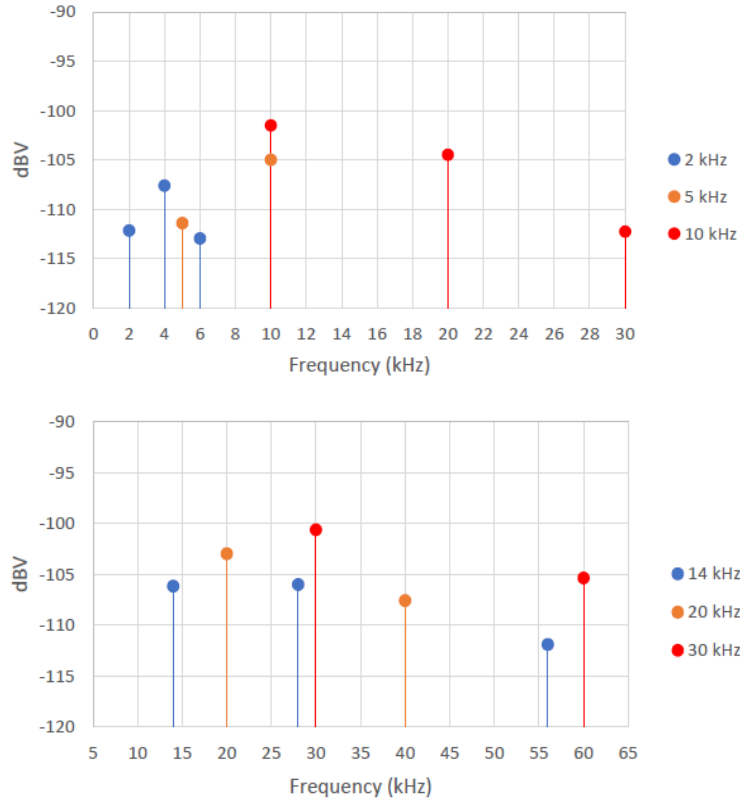
Note the presence of the third harmonic at the 10 kHz drive.

Figure 36.   Frequency spectra of the low-density CNT sheet
at various driving frequencies.

For the narrow low-density CNT sheet, the second harmonic had a much stronger RMS pressure response than the first harmonic at frequencies below 2 kHz. Looking at the frequency spectra in Figure 37, the difference between the first and second harmonic for a 2 kHz or 5kHz drive is about 6 dBV. In addition, the values of the first harmonic for 2 kHz and 5 kHz are above those of the high-density sheet and below those of the low-density sheet. However, the narrow sheet has the largest values for the second harmonic at low frequencies.
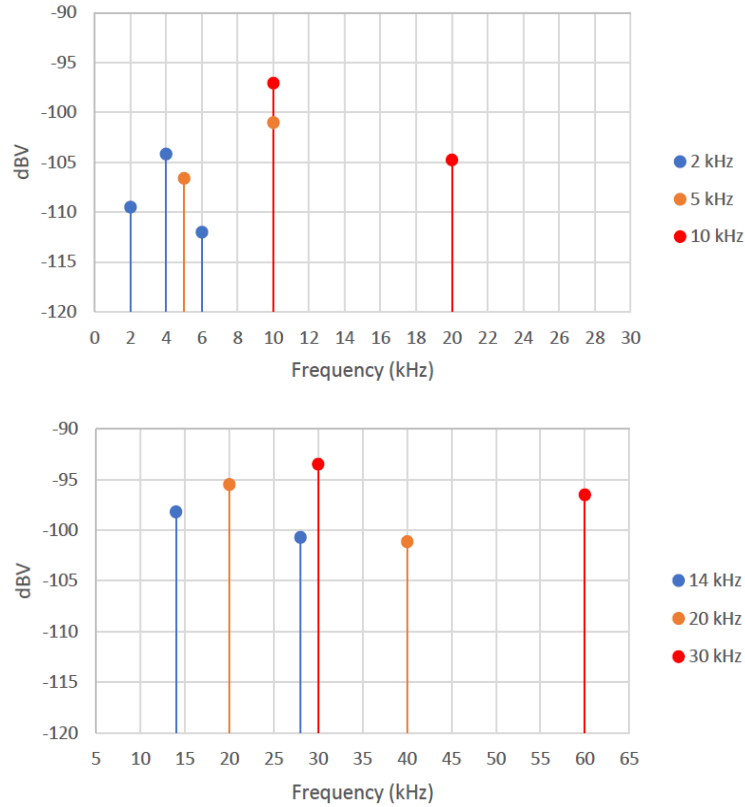
Figure 37.　　　Frequency spectrum of the narrow low-density sheet.

These thermophones do not exhibit the double frequency effect at 10 kHz or above. This is most likely due to the impedance mismatch in the circuit. Since power is not being delivered optimally, the second harmonic is not appearing as stronger than the first harmonic at higher frequencies. At the lower frequencies of 2 kHz and 5 kHz, the CNT sheet is still in the purely resistive regime. However, the power being delivered is not enough to counteract the increased reactance of the CNT at frequencies above 10 kHz.

The frequency spectrum of the final thermophone iteration differs from the previous three. At all drive frequencies except 2 kHz, the second harmonic has a stronger response than the first harmonic. This fact is no surprise given the wider frequency range over which the RMS pressure follows the theory (Figure 38).
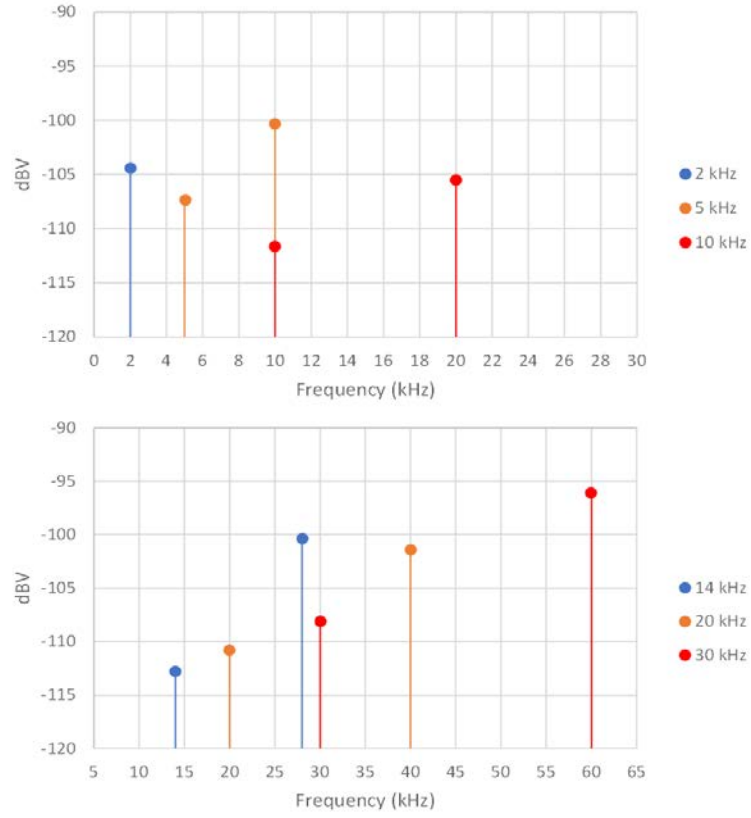
Note the higher second harmonic at each drive frequency.

Figure 38.   Frequency spectrum of the low mass narrow sheet.

THIS PAGE INTENTIONALLY LEFT BLANK

V. FUTURE WORK AND APPLICATIONS

This thesis has shown that Miralon® sheets from Nanocomp are a viable material for CNT based TA devices. The next step for this material is to go beyond the basic acoustic characterization that has been done in this thesis and apply it to TA devices that have already been built and tested. The most promising application of CNT based thermophones for the U.S Navy is lightweight SONAR projectors. N. Mayo et al have developed this technology at the Naval Undersea Warfare Center (NUWC) Newport division. Their work involves encapsulating CNT films in liquids and gas to be used underwater (Figure 39). According to their research, encapsulating a TA material creates a more resonant system that can be custom made for its intended use environment [9]. The material used in the NUWC tests is similar to the thin films used by Lin et al. However, the Miralon® sheets could potentially be used in the same way since they are easy to cut and shape for a variety of applications.
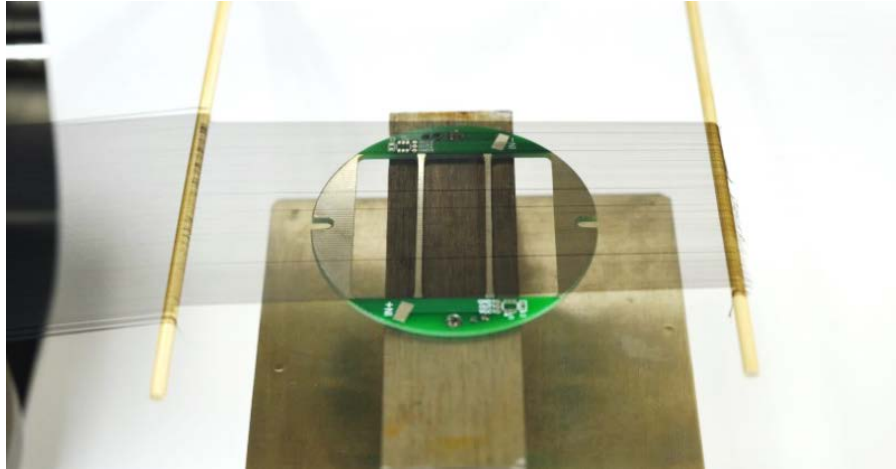
Figure 39.   Thin CNT film being drawn across
a casing to be encapsulated. Source: [9].

Encapsulated thermophones are just one possible use for Miralon® sheets in the TA field. Their flexibility allows them to be used in virtually any capacity as a TA material, with performance comparable to other CNT based TA materials tested. Further testing in

an acoustically isolated environment and in an impedance matched circuit will reveal the true potential of Miralon® sheets. The field of TA has experienced a revival thanks to CNT based materials, and Miralon® sheets can certainly be a part of a new type of acoustic devices based on this technology.

APPENDIX. MATERIAL PROPERTIES

A.   MIRALON® SHEETS

Nanocomp supplied two Miralon® sheets. One had a density of 10–15 gsm and the other had a density of 20–30 gsm. Table 1 shows the material properties of the 10–15 gsm sheet provided by Nanocomp. Other than the difference in density, it is assumed that the 20–30 gsm sheet has the same material properties.

Table 1.   Physical Properties of 10–15 gsm sheet. Adapted from [6].

Property	Units
Bulk Density	0.3–0.5 g/cm^3
Areal Density	10–15 g/m^2
Thickness	22 um
Standard Widths	0.64–137 cm
Porosity	70%
Temperature Operating Range	-200 to +250 C
Max Processing Temperature	350 C
Thermal Conductivity	30 W/m K
CTE	-3x10^-6 m/m C
Surface Resistivity	1.5 Ohms/square
Specific Conductivity	600 S cm^2 / g
Specific Strength	0.07 GPa / (g/cm^3)

B. MICROPHONE DATA

1. Larson Davis Model 2530

Table 2. Larson Davis Model 2530 specifications.

Property	Units
Nominal Diameter	1/4 in
Open Circuit Frequency Response (± 2dB)	4 Hz to 70 kHz
Open Circuit Sensitivity (250 Hz)	1.45 mV/Pa (-56.7 ± 2 dB re 1 V/Pa)

2. B&K Model 4138

Table 3. B&K Model 4138 specifications.

Property	Units
Nominal Diameter	1/8 in
Open Circuit Frequency Response (± 2dB)	6.5 Hz to 140 kHz
Open Circuit Sensitivity (250 Hz)	1 mV/Pa (-60 ± 1.5 dB re 1 V/Pa)

LIST OF REFERENCES

[1]   H. D. Arnold and I. B. Crandall, "The thermophone as a precision source of sound," *Phys. Rev*. vol. 10, no. 1, pp. 22-38, Jul. 1, 1917. [Online]. Available: https://doi.org/10.1103/PhysRev.10.22

[2]   N. Mayo, "Advancements in thermophones: Sound generation from nanoscopic heaters," *Acoustics Today*, vol. 14, no. 4, pp. 47–55. 2018. [Online]. Available: https://acousticstoday.org/wp-content/uploads/2018/12/Advancements-in-Thermophones-Nathanael-Mayo.pdf

[3]   A. R. Barnard, M. Asgarisabet, and T. Bouman, "The carbon nanotube thermophone: A near-weightless audio driver with no moving parts," presented at ALMA International, Las Vegas, NV, Jan. 2, 2016.

[4]   Xiao Lin et al (2008). "Flexible, stretchable, transparent carbon nanotube thin film loudspeakers," *Nano Letters*, vol. 8, no. 12, pp. 4539-4545, 2008. [Online]. Available: https://doi.org/10.1021/nl802750z

[5]   A. E. Aliev, "Thermophones using carbon nanotubes and alternative nanostructures for high power sound generation and noise cancellation," presented at Inter-Noise, Melbourne, Australia, 16-19 November, 2014.

[6]   "Problems of transducer design," class notes to Sonar Transducers, Dept. of Physics, Naval Postgraduate School, Monterey, CA, USA, winter 2019

[7]   L. Freznel, "Back to basics: impedance matching (part 1)," Electronic Design, October 24, 2011. [Online]. Available. https://www.electronicdesign.com/communications/back-basics-impedance-matching-part-1

[8]   A. E. Aliev, M. D. Lima, S. Fang, and R. H. Baughman, "Underwater sound generation using carbon nanotube projectors," *Nano Letters,* vol. 10, no. 7, pp 2374-2380, May 2010 [Online]. doi: 10.1021/nl100235n

[9]   N. Mayo et al, "Thermophones for sonar applications," presented at 174th meeting of the Acoustical Society of America, New Orleans. LA, Dec. 5, 2017.

THIS PAGE INTENTIONALLY LEFT BLANK

INITIAL DISTRIBUTION LIST

1.   Defense Technical Information Center
        Ft. Belvoir, Virginia

2.   Dudley Knox Library
        Naval Postgraduate School
        Monterey, California